



OPEN The Sarcoplasmic/Endoplasmic reticulum Ca^{2+} -ATPase (SERCA) is present in pig sperm and modulates their physiology over liquid preservation

Ferran Garriga^{1,2}, Jesús Martínez-Hernández^{1,2,3}, Ainhoa Parra-Balaguer^{1,2}, Marc Llavanera^{4,6}✉ & Marc Yeste^{1,2,5,6}✉

Liquid storage is the primary preservation method in the swine breeding industry because of its advantages over cryopreservation. Calcium (Ca^{2+}), a key regulator of cell physiology, plays a crucial role during liquid preservation. Sarcoplasmic/Endoplasmic Reticulum Ca^{2+} ATPases (SERCA) belong to a family of P-type ATPases that regulate Ca^{2+} homeostasis within cells and have been previously described to play a function in the sperm of various mammalian species. Herein, we hypothesized that SERCA2 is present in pig sperm and is involved in the resilience of this cell to liquid preservation at 17 °C. For this purpose, sperm were incubated with different concentrations of thapsigargin (Thg; 0, 5, 25, and 50 μM) and stored at 17 °C for ten days. The presence and localization of SERCA2 were evaluated using immunoblotting and immunofluorescence, respectively. On days 0, 4, and 10, sperm motility was assessed using a computer-assisted sperm analysis (CASA) system, and sperm viability, membrane lipid disorder, acrosome integrity, mitochondrial membrane potential (MMP), and intracellular levels of Ca^{2+} , superoxides and total reactive oxygen species (ROS) were evaluated by flow cytometry. We localized SERCA2 in the acrosome and midpiece of pig sperm. Furthermore, inhibition of SERCA with Thg resulted in reduced sperm viability and membrane stability, and increased MMP, and Ca^{2+} and ROS levels. In conclusion, the activity of SERCA prevents the accumulation of intracellular Ca^{2+} in sperm, which is detrimental to sperm quality and function during liquid storage at 17 °C. We thus suggest that the function of SERCA is crucial for the preservation of pig semen.

Keywords Semen, Pig, Liquid storage, SERCA, Thapsigargin, Calcium

Abbreviations

AI	Artificial Insemination
ALH	Amplitude of Lateral Head displacement
BCF	Beat-Cross Frequency
Ca^{2+}	Calcium
CASA	Computer-Assisted Sperm Analysis
CLSM	Confocal Laser-Scanning Microscope
FSD	Forward Scatter Detector
H_2DCFDA	Dichlorodihydrofluorescein diacetate
HE	Dihydroethidium
ISAS	Integrated Sperm Analysis System

¹Biotechnology of Animal and Human Reproduction (TechnoSperm), Institute of Food and Agricultural Technology, University of Girona, Girona 17003, Spain. ²Unit of Cell Biology, Department of Biology, Faculty of Sciences, University of Girona, Girona 17003, Spain. ³Department of Cell Biology and Histology, Faculty of Medicine, Regional Campus of International Excellence "Campus Mare Nostrum", IMIB-Arixaca, University of Murcia, Murcia 30120, Spain. ⁴Laboratory of Chromosome Biology, Max Planck Institute of Biochemistry, 82152 Martinsried, Germany. ⁵Catalan Institution for Research and Advanced Studies (ICREA), Barcelona 08010, Spain. ⁶Marc Llavanera and Marc Yeste have share senior authorship. ✉email: llavanera@biochem.mpg.de; marc.yeste@udg.edu

JC-1 _{agg}	JC-1 aggregates
JC-1 _{mon}	JC-1 monomers
LD	LIVE/DEAD™ Fixable Far Red
LIN	Linearity
M540	Merocyanine 540
MMP	Mitochondrial Membrane Potential
PI	Propidium Iodide
PNA	Arachys hypogaea peanut lectin
ROS	Reactive Oxygen Species
SERCA	Sarcoplasmic/Endoplasmic Ca ²⁺ ATPase
SSD	Side Scatter Detector
STR	Straightness
Thg	Thapsigargin
VAP	Average-path velocity
VCL	Curvilinear velocity
VSL	Straight-line velocity
WOB	Wobble

Sperm preservation before artificial insemination (AI) is a critical step in the swine breeding industry, as it is essential for maintaining the function and survival of the male gamete¹. Although two main preservation methods - cryopreservation and liquid storage - are available, 99% of AI in swine utilize liquid-stored semen². This preference for liquid sperm storage is due to its ability to maintain sperm quality and fertilizing ability better than cryopreservation, which is known to impair their functionality and reduce their reproductive performance³. The main limitation of liquid storage, however, is the restricted period over which sperm can be preserved. As pig sperm are susceptible to low temperatures⁴, storing is typically carried out at temperatures between 15 and 20 °C⁵. At this range, nevertheless, the extent to which sperm metabolism can be reduced is smaller than at lower temperatures like 4–5 °C, making the preservation of these cells more difficult.

Calcium (Ca²⁺) has consistently been shown to be crucial for sperm physiology^{6–9}. Intracellular Ca²⁺ levels and Ca²⁺ channels have been reported to play a critical role in regulating mammalian sperm motility^{10,11}. Moreover, not only is Ca²⁺ highly relevant for the induction and regulation of sperm capacitation and acrosome reaction in mammals^{12–15}, but also for the activation of the oocyte upon fertilization^{16,17}. Regarding sperm preservation, Ca²⁺ has been particularly related to the maintenance of sperm over liquid storage. Indeed, previous studies associated high intracellular Ca²⁺ levels with a decrease in sperm viability during preservation of pig sperm at 15–20 °C^{18,19}. Besides, higher Ca²⁺ levels in pig sperm are correlated to a reduction in the litter size, notwithstanding the molecular mechanisms underlying this relationship need to be investigated further²⁰.

Considering the vital role of Ca²⁺ in sperm physiology, the study of proteins that regulate Ca²⁺ in sperm is of high interest. Sarcoplasmic/Endoplasmic Reticulum Ca²⁺-ATPases (SERCA) is a family of Ca²⁺ pumps that, in somatic cells, transport Ca²⁺ from the cytosol to the endoplasmic reticulum²¹. Three genes encode this protein family: *SERCA1*, *SERCA2* and *SERCA3*, with the second one being expressed in most tissues. Although mature sperm do not have endoplasmic reticulum, the presence of *SERCA2* was described in human, bovine and mouse sperm²², particularly in the acrosome and midpiece. Yet, and to the best of our knowledge, its presence in pig sperm has not been interrogated.

Thapsigargin (Thg), a drug compound derived from the plant *Thapsia garganica*, is a well-known, specific inhibitor of SERCA family isoforms²³. Incubation of cancer cells with Thg was found to induce cell death through the depletion of endoplasmic reticulum Ca²⁺ stores²⁴. Regarding its effect on sperm, Thg was observed to boost intracellular Ca²⁺ in humans, which was seen to result from the depletion of internal Ca²⁺ stores and the opening of Ca²⁺ channels of the plasma membrane. This was reported to lead to an increase in the occurrence of the acrosome reaction and a decrease in sperm motility^{25–27}. In pigs, Thg was established to increase intracellular Ca²⁺, especially in fresh compared to cryopreserved sperm²⁸. Furthermore, incubation with Thg was seen to induce head-to-head agglutination, which would suggest that SERCA activity is involved in capacitation-like changes mediated by Ca²⁺²⁹. Despite this, no previous study has investigated the presence of SERCA in pig sperm, nor has it evaluated how inhibiting SERCA through Thg affects their resilience to liquid storage.

In light of the aforementioned, two objectives were set in the present work: (1) to determine the presence and localization of *SERCA2* in pig sperm; and (2) to elucidate the role of SERCA, by their inhibition with Thg, in the maintenance of sperm quality and functionality during liquid storage at 17 °C. We hypothesize that SERCA are present in pig sperm and are involved in keeping them in good shape over preservation at 17 °C.

Results

SERCA2 is present in pig sperm and localizes at the acrosome and the midpiece

Immunoblotting with the anti-SERCA2 antibody revealed three predominant bands of 50, 75 and 110 kDa (Fig. 1A). The specificity of the SERCA2-bands was confirmed through a competition assay with the recombinant protein, and a negative control lacking the primary antibody (Supplementary Fig. S1). Neither in the competition assay with the recombinant protein nor in the negative control were the 75 kDa and 110 kDa bands present, whereas that of 50 kDa was observed in the two controls.

Immunofluorescence analysis revealed that, in pig sperm, SERCA2 is primarily localized in the acrosome and midpiece (Fig. 1B). Besides, weaker SERCA2 expression was observed in the post-acrosomal region of some sperm cells. No SERCA2 signal was detected in the competition assay with the recombinant protein or the negative control (Supplementary Fig. S2).

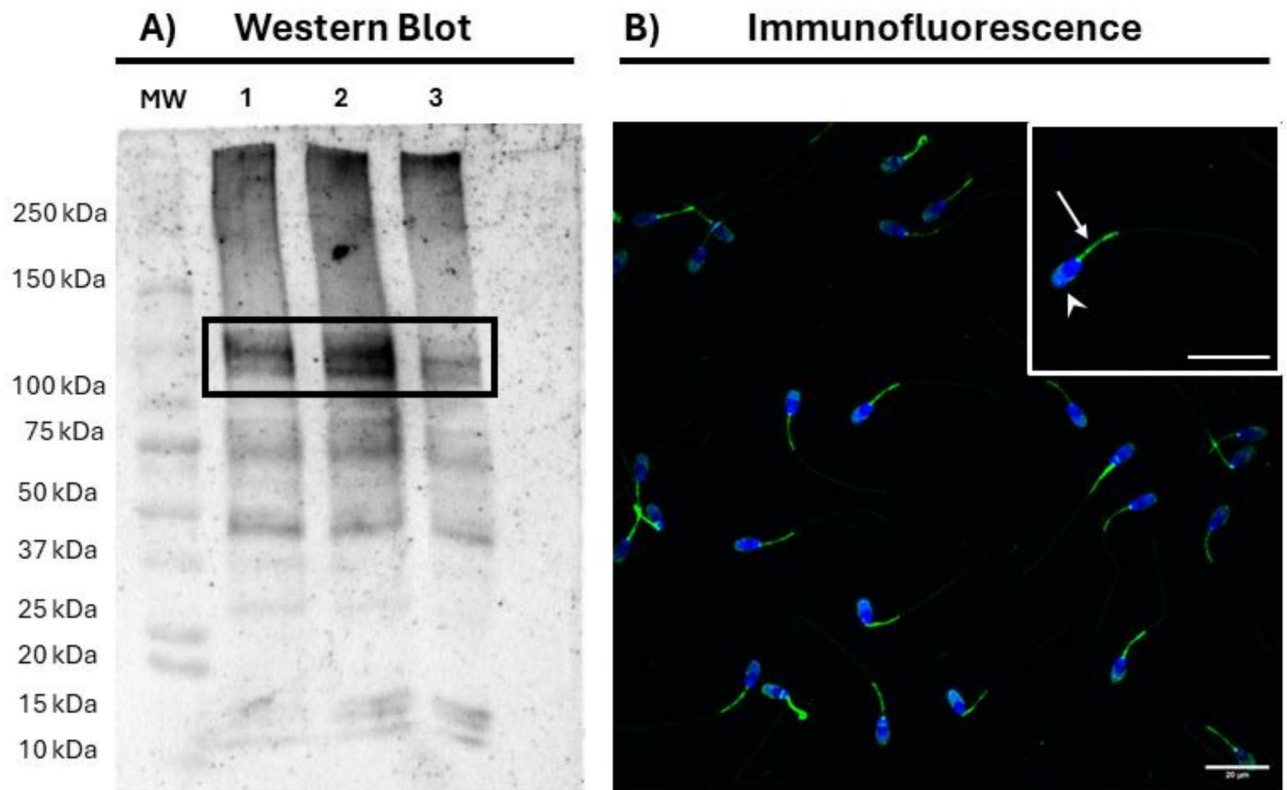


Fig. 1. Presence and localization of SERCA2 in pig sperm. (a) Representative immunoblotting of SERCA2 in pig sperm after incubation with the anti-SERCA2 antibody. MW: Molecular Weight; 1–3 correspond to different samples. The black box indicates the SERCA2 band. (b) Representative immunofluorescence analysis of SERCA2 in pig sperm. Sperm nuclei are shown in blue (DAPI), whereas SERCA2 is shown in green. The white arrow shows the localization of SERCA2 in the midpiece, whereas arrowheads show its presence in the acrosome. Scale bars: 20 μm .

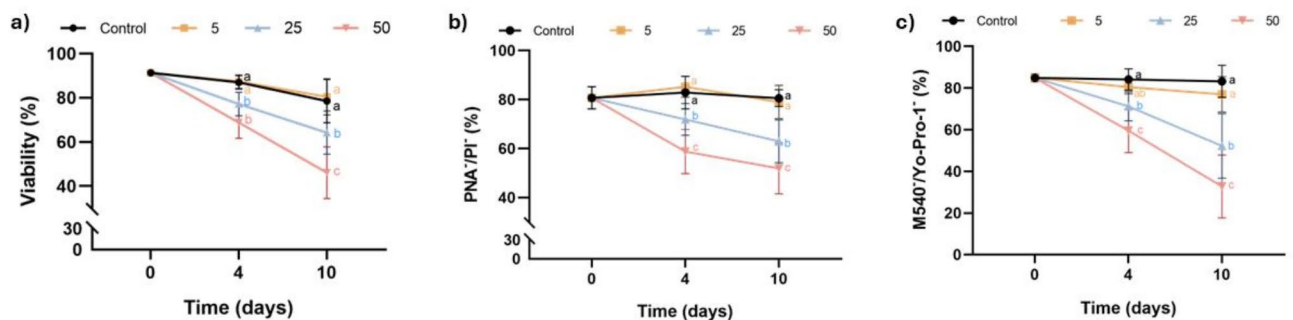


Fig. 2. Effect of inhibiting SERCA activity with Thg on the plasma membrane and acrosome integrity, and lipid membrane stability. (a) Viable sperm (SYBR-14⁺/PI⁻, %); (b) viable sperm with an intact acrosome (PNA⁻/PI⁻, %); and (c) viable sperm with high lipid membrane stability (M5407Yo-Pro-1⁻, %) after 0, 4 and 10 days of liquid storage at 17 °C in the presence (5, 25 and 50 μM) or absence (0 μM ; control) of Thg. Different letters (a–c) indicate significant differences between experimental groups at a given time point. Results are expressed as the mean \pm SEM ($n = 7$).

Inhibition of SERCA compromises plasma membrane and acrosome integrity during liquid storage of pig sperm

The effects of inhibiting SERCA with Thg during liquid preservation at 17 °C of pig semen are shown in Fig. 2 and Supplementary File 2. Regarding sperm viability, and as Fig. 2a shows, the blockage of SERCA with 25 μM and 50 μM Thg led to a decrease in the percentage of viable sperm ($P < 0.05$; SYBR-14⁺/PI⁻) after 4 and 10 days of storage at 17 °C. Concerning acrosome integrity (Fig. 2b), inhibiting SERCA with 25 μM and 50 μM Thg reduced ($P < 0.05$) the percentage of viable sperm with an intact acrosome (PNA⁻/PI⁻) after 4 and 10 days of storage.

Similar results were observed in the case of lipid membrane stability, as the inhibition of SERCA activity with Thg (25 μM and 50 μM) decreased the percentage of viable sperm ($P < 0.05$) with high lipid membrane stability (M540⁻/Yo-Pro-1⁻) after 4 and 10 days of storage (Fig. 2c). Noticeably, in the three variables, the effects were similar and dose-dependent, with no change at 5 μM and the most significant impact at 50 μM .

Inhibition of SERCA with Thg increases ROS levels in liquid-stored sperm

Intracellular levels of superoxides and total ROS were assessed using a double-staining with HE/Yo-Pro-1 and H₂DCFDA/PI, respectively. Figure 3a shows the E⁺ intensity in viable sperm, normalized to the control. Incubation with 25 μM and 50 μM Thg significantly increased intracellular superoxide levels after 4 days of storage ($P < 0.05$); these differences were not observed at day 10. Regarding total ROS levels, Fig. 3b depicts the DCF⁺ fluorescence intensity, normalized to the control. Inhibiting SERCA with 5 μM Thg, but not with higher concentrations of this molecule (25 μM or 50 μM), increased the levels of total ROS after 4 days of storage ($P < 0.05$). This effect, however, was not observed after 10 days of storage.

Inhibition of SERCA with thapsigargin increases mitochondrial activity and Ca²⁺ levels in liquid-stored sperm

Intracellular Ca²⁺ levels were measured by the intensity of Fluo4 in viable sperm, normalized to the control (Fig. 4a). Incubation with 25 μM and 50 μM Thg resulted in a significant increase in intracellular Ca²⁺ levels at day 4, with only the highest concentration maintaining this effect at day 10 ($P < 0.05$). On the other hand, mitochondrial membrane potential was assessed using a double staining protocol with JC-1 and LD. The results, shown in Fig. 4b, were expressed as the ratio between JC-1_{agg} and JC-1_{mon}. Incubation of pig sperm with the highest concentration of Thg (50 μM) significantly raised the mitochondrial membrane potential at both days 4 and 10 ($P < 0.05$), whereas the other two concentrations (5 μM and 25 μM) had no effect ($P > 0.05$).

Sperm motility and kinematics are not affected by SERCA inhibition during liquid storage of pig sperm

Figure 5 illustrates the percentages of total motile sperm (Fig. 5a) and progressively motile sperm (Fig. 5b). Incubation with Thg did not affect these percentages at any of the time points and concentrations assessed ($P > 0.05$). Furthermore, Table 1 displays the impact of inhibiting SERCA on the kinematic parameters of pig sperm during liquid storage at 17 °C. No significant differences were observed between experimental groups for any of the analyzed parameters ($P > 0.05$).

Discussion

In pigs, semen preservation ahead of AI primarily relies on liquid storage due to the limitations of cryopreservation⁵. Ca²⁺ is a well-known regulator of sperm physiology, and its involvement in keeping sperm in good shape during liquid storage has been previously documented^{8,18,19}. Consequently, studying the molecular mechanisms regulating Ca²⁺ homeostasis in pig sperm is particularly interesting. Related to this, SERCA are a family of pumps that mediate the intracellular Ca²⁺ transport²¹. While the presence of SERCA in the sperm of various mammalian species has been investigated, their localization and role in pig sperm have not been explored, despite their potential relevance for liquid preservation²². The present study, therefore, sought to

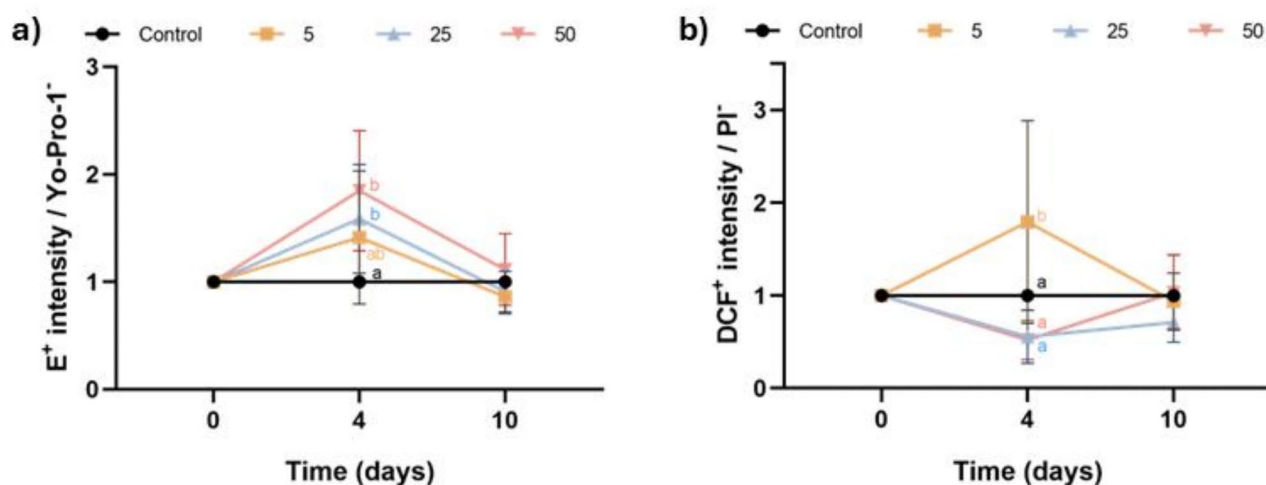


Fig. 3. Effect of inhibiting SERCA activity with Thg on reactive oxygen species (ROS) levels. (a) E⁺ intensity in viable sperm (Yo-Pro-1⁻); and (b) DCF⁺ intensity in viable sperm (PI⁻) after 0, 4 and 10 days of liquid storage at 17 °C in the presence (5, 25 and 50 μM) or absence (0 μM ; control) of Thg. Different letters (a-c) indicate significant differences between experimental groups at a given time point. Results are expressed as the mean \pm SEM ($n = 7$).

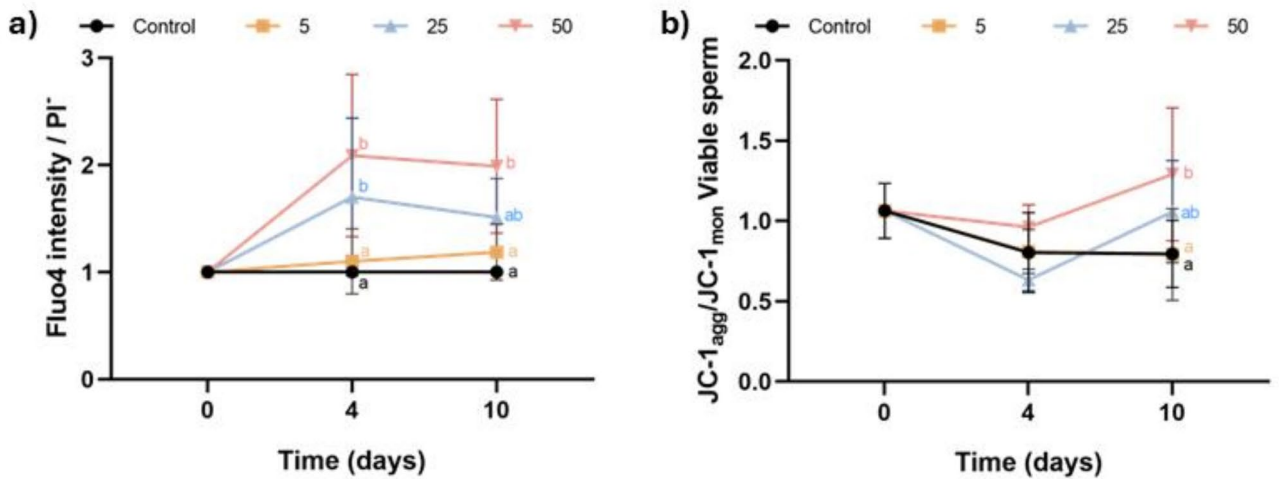


Fig. 4. Effect of inhibiting SERCA activity with Thg on intracellular calcium (Ca^{2+}) and mitochondrial membrane potential (MMP). (a) Fluo4 intensity in viable sperm (PI^-); and (b) ratio between JC-1_{agg} and JC-1_{mon} in viable sperm (LD^-) after 0, 4 and 10 days of liquid storage at 17 °C in the presence (5, 25 and 50 μM) or absence (0 μM; control) of Thg. Different letters (a-c) indicate significant differences between experimental groups at a given time point. Results are expressed as the mean \pm SEM ($n=7$).

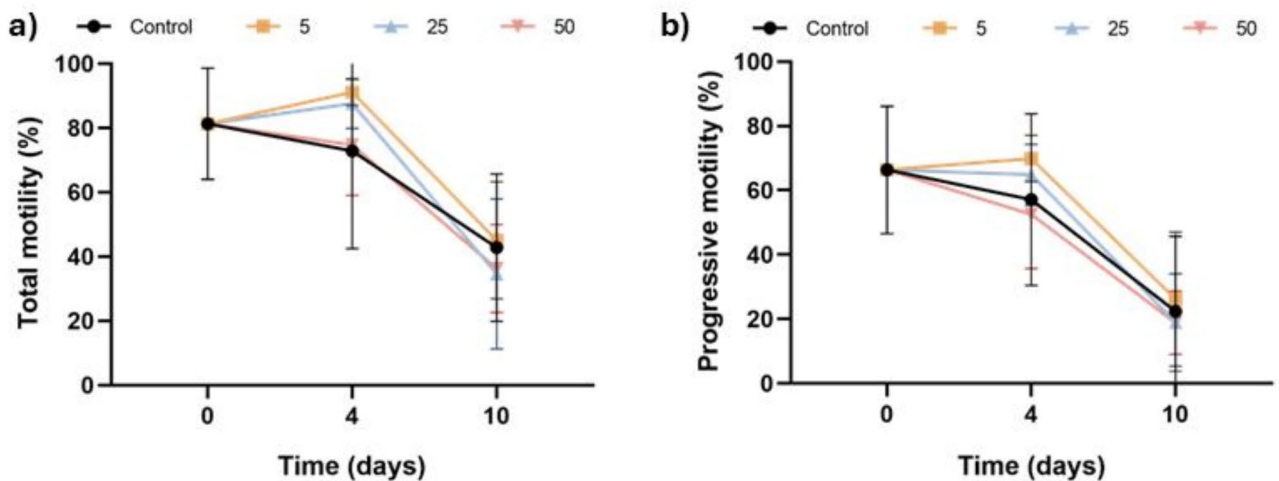


Fig. 5. Effect of inhibiting SERCA activity with Thg on sperm motility. (a) Percentages of total motile sperm; and (b) percentages of progressively motile sperm after 0, 4 and 10 days of liquid storage at 17 °C in the presence (5, 25 and 50 μM) or absence (0 μM; control) of Thg. No significant differences between groups were observed. Results are expressed as the mean \pm SEM ($n=7$).

determine the presence and localization of SERCA2 in pig sperm as well as elucidate the role of these Ca^{2+} pumps in maintaining their function and survival during liquid storage at 17 °C.

We first assessed the presence of SERCA2 in pig sperm through immunoblotting. Two SERCA2-specific bands of ~75 and ~110 kDa were observed in the blots. Besides, a ~50-kDa band was observed in the same blots, but it was determined to be nonspecific to SERCA2, as it also appeared in both the competition assay with the recombinant SERCA2 and the negative control without the primary antibody. It is worth noting that the ~110-kDa band coincides with the molecular weight of SERCA2, which is known to be between 110 and 115 kDa³⁰. In contrast, the ~75-kDa band, though specific to SERCA2, has not been previously reported and could be an alternative isoform resulting from splicing events. Further studies are, however, necessary to confirm this suggestion. Remarkably, the presence of a 110-kDa band in porcine sperm aligns with previous studies that identified SERCA2 in human, bovine and murine sperm²². Taken together, these results suggest that SERCA2 is present and conserved across the sperm of different mammalian species.

Immunofluorescence analysis was carried out to localize SERCA2 in pig sperm, revealing that this protein resides in the acrosome and midpiece of pig sperm. This localization pattern agrees with previous findings in other mammalian species. In human sperm, SERCA2 exhibits a similar localization pattern as that observed

in porcine sperm in the present study²². Conversely, in bovine and murine sperm, SERCA2 is localized in the acrosome but not in the midpiece²². These findings again suggest a conserved localization pattern for SERCA2 across mammalian sperm.

After confirming the presence and localizing SERCA2 in porcine sperm, we aimed to determine the role of SERCA in the maintenance of sperm quality during liquid storage at 17 °C; for this purpose, SERCA were specifically inhibited with Thg. One of the most notable effects of inhibiting SERCA during liquid preservation of pig sperm was the impairment of plasma and acrosome integrity, suggesting that the activity of these pumps is essential for maintaining sperm viability and keeping the acrosome intact over storage at 17 °C. Thapsigargin has been described to induce cell death through depleting Ca²⁺ in the endoplasmic reticulum of other cell types^{24,31}. While mature sperm lack the endoplasmic reticulum, the negative impact of Thg on their viability has also been reported in human sperm²⁷, likely due to increased intracellular Ca²⁺ levels. An overload of intracellular Ca²⁺ might lead to the activation of cell death pathways, thus compromising sperm viability^{32–34}. Specifically, an increase in Fluo4 intensity has been previously associated with reduced sperm viability during liquid storage of pig sperm¹⁸, suggesting a critical relationship between Ca²⁺ homeostasis and sperm viability.

On the other hand, how inhibiting SERCA with Thg affects acrosome integrity has been extensively documented. In capacitated human and mouse sperm, Thg was identified as an inducer of the acrosome reaction^{25,35}. This is consistent with the established role of the acrosome as an important Ca²⁺ reservoir^{26,36,37}. Considering the localization pattern of SERCA2 described in this and other studies, one could suggest that the active Ca²⁺ transport into the acrosome is regulated by SERCA²². This hypothesis would be supported by a previous study showing that incubating non-capacitated human sperm with Thg increases the percentages of viable sperm undergoing acrosome reaction and those of non-viable sperm with an exocytosed acrosome²⁷. The ability to induce the acrosome reaction in capacitated sperm is understood to rely upon the Ca²⁺ entry from the external medium^{26,38}. Thus, one may reasonably suggest that SERCA play a role in preventing spontaneous acrosome exocytosis during liquid preservation of pig sperm by maintaining Ca²⁺ homeostasis.

Regarding the influence of SERCA activity in the architecture of the sperm plasma membrane, inhibition of SERCA with Thg resulted in a decrease in lipid membrane stability. While, to the best of our knowledge, there is no previous literature specifically addressing the effect of Thg on the lipid disorder of sperm plasmalemma, the decrease in lipid membrane stability observed herein after blocking the SERCA could be related to the detrimental impact on sperm viability and acrosome integrity mentioned above. M540 incorporation into the plasma membrane of mammalian sperm is associated to the first stages of sperm capacitation³⁹, suggesting that inhibiting SERCA with Thg may trigger capacitation-like changes during liquid storage of pig sperm⁴⁰. This aligns with our hypothesis that SERCA are critical to prevent premature sperm capacitation and acrosome exocytosis under these conditions. Nevertheless, further research is required to fully elucidate the connection between the inhibition of SERCA by Thg and the occurrence of capacitation-like changes.

One of the most notable effects of blocking SERCA on pig sperm was the increase in intracellular Ca²⁺ levels. It is well documented that inhibiting SERCA activity with Thg induces a rise in intracellular Ca²⁺ levels. Two mechanisms have been described for this effect. First, Thg leads to the depletion of intercellular Ca²⁺ stores²⁶. Second, SERCA inhibition is also known to trigger Ca²⁺ entry from the extracellular medium in capacitated sperm^{27,38}. As Fluo4 stains the overall intracellular Ca²⁺¹⁸, the increase observed in the present study could result from an extracellular Ca²⁺ influx. Hence, not only do SERCA regulate intracellular Ca²⁺ transport but they may also influence the capacitating extracellular Ca²⁺ uptake, suggesting a potential role in the activation of stored-operated Ca²⁺ entry (SOCE). Store-operated Ca²⁺, which are activated in somatic cells upon depletion of Ca²⁺ from the endoplasmic reticulum⁴¹, mediate capacitating Ca²⁺ entry from the extracellular medium^{42,43}. While the presence of ORAI and STIM, which are key components of SOCE, has been identified in sperm⁴⁴, further research is required to clarify the specific role these channels play in sperm function. As previously noted, Ca²⁺ is crucial in regulating sperm physiology under various conditions^{8,11,15}. Hence, the observed intracellular Ca²⁺ overload could provide an explanation for the detrimental effects on sperm viability, membrane stability, and acrosome integrity.

Although how blocking SERCA affects mitochondrial activity was not previously interrogated, our findings indicated that inhibiting the activity of these pumps during liquid storage increases the MMP of pig sperm. In addition to all the aforementioned, Ca²⁺ is known to be an important regulator of mitochondrial activity, acting as a secondary messenger in various mitochondrial functions, including ATP production⁴⁵. While, to the best of our knowledge, the current literature does not establish a direct link between high intracellular Ca²⁺ levels and elevated MMP in sperm, the results of the present study suggest that Ca²⁺ homeostasis could influence the mitochondrial activity in pig sperm. Nevertheless, further research is required to elucidate this association and the molecular mechanisms involved in this regulation. Concerning the effect of inhibiting SERCA on ROS levels, the incubation of sperm with Thg increased both superoxide and total ROS levels, but this was observed only at day 4 of storage. This effect could be tightly related to the previously described increase in MMP, as mitochondria are widely understood as a major source of ROS in sperm^{46,47}. The observed rise in mitochondrial activity could thus be responsible for the increased intracellular ROS levels.

Finally, blocking SERCA activity during liquid storage had no effect on sperm motility, as neither the percentages of total and progressively motile sperm nor kinematic parameters were affected by the different concentrations of Thg. These findings contrasted with a previous study in humans, where incubation of sperm with Thg resulted in a rapid reduction of sperm motility²⁷. The decrease in motility was attributed to an overload of intracellular Ca²⁺, which may inhibit sperm motility⁴⁸. Despite observing an increase in intracellular Ca²⁺ in our study, the same impact on sperm motility was not detected. This would open the possibility that, in liquid-stored sperm - and in contrast to capacitated sperm where the PKC pathway plays a vital role -, the function of Ca²⁺ in the regulation of sperm motility is different. Nevertheless, further research is needed to better understand the relationship between Ca²⁺ and motility in liquid-stored sperm, as well as the role of SERCA.

Conclusions

In conclusion, this study has confirmed the presence and reported the localization of SERCA2 in pig sperm, which resides in the acrosome and the midpiece. Furthermore, it has demonstrated that Ca^{2+} homeostasis during liquid storage is essential for preserving sperm function and survival, and that SERCA are crucial for that homeostasis, given their relevance for sperm viability and acrosome integrity and because they prevent excessive mitochondrial activity and ROS levels. Our study contributes to increase the knowledge base on the molecular mechanisms regulating the maintenance of sperm during liquid preservation. Moreover, it opens the door to further research, investigating whether semen aging during liquid preservation is, among other factors, caused by impaired SERCA function. This highlights the need to explore other proteins involved in the regulation of intracellular Ca^{2+} .

Methods

Samples and experimental design

Semen samples from seven healthy and sexually mature boars were used in the present work. Samples were provided by an artificial insemination center (Grup Gepork, S.A.; Masies de Roda, Spain), which fed animals under controlled conditions and held adequate permissions to sell seminal doses. As the authors of this study did not manipulate any animal and seminal doses were commercial, no approval from an Ethics committee was required. Seminal doses were diluted to 33×10^6 sperm per mL in a final volume of 90 mL of a commercial extender (Vitasem LD; Magapor, S.L.; Zaragoza, Spain). Samples were then cooled to 17 °C and transported to our laboratory within the first 24 h post-collection. Upon arrival, every sample was divided into four aliquots and subsequently incubated at 17 °C for ten days with different concentrations of Thg (0, 5, 25, and 50 μM). Sperm parameters were assessed on days 0, 4, and 10.

Sperm motility

Sperm motility was evaluated using a computer-assisted sperm analysis (CASA) system, consisting of a phase-contrast microscope (Olympus BX41; Olympus, Tokyo, Japan) equipped with a camera and the Integrated Sperm Analysis System (ISAS; V1.0; Proiser, S.L.; Valencia, Spain) software. Samples were incubated at 38 °C for 5 min and placed in a pre-warmed Leja chamber (Leja Products BV; Nieuw-Vennep, The Netherlands). A total of 1,000 sperm per sample were captured. Percentages of total motile sperm (%) and progressively motile sperm (%) were recorded for each sample, as well as the following kinematic parameters: curvilinear velocity (VCL, $\mu\text{m/s}$), straight-line velocity (VSL, $\mu\text{m/s}$); average-path velocity (VAP, $\mu\text{m/s}$), linearity (LIN, %), straightness (STR, %), wobble (WOB, %), amplitude of lateral head displacement (ALH, μm) and beat-cross frequency (BCF, Hz). Sperm with a VAP equal to or greater than 10 $\mu\text{m/s}$ were considered motile and those with a STR equal to or higher than 45% were considered progressively motile. Twenty-five images per second were captured, and settings were configured as follows: only particles between 10 and 80 μm^2 were analyzed, connectivity was set to 11, and at least 10 images were required to calculate the ALH.

Flow cytometry

A CytoFlex flow cytometer (Beckman Coulter; Brea, CA, USA) was used to evaluate sperm functionality parameters: sperm viability (SYBR-14/propidium iodide [PI]), lipid membrane disorder (merocyanine 540 [M540]/Yo-Pro-1), acrosome integrity (*Arachis hypogaea* peanut lectin [PNA]/PI), mitochondrial membrane potential (JC-1/[LIVE/DEAD™ Fixable Far Red]), intracellular superoxide levels (dihydroethidium [HE]/Yo-Pro-1), intracellular total ROS levels (dichlorodihydrofluorescein diacetate [H_2DCFDA]/PI) and intracellular Ca^{2+} levels (Fluo4-AM/PI).

The Forward Scatter Detector (FSD) and the Side Scatter Detector (SSD) were used to gate the sperm population. All fluorochromes were excited at 488 nm, except LIVE/DEAD™ Fixable Far Red (LD), which was excited at 638 nm. The fluorescence from SYBR-14, Yo-Pro-1, PNA-FITC, DCF, Fluo4, and JC-1 monomers (JC-1_{mon}) was detected through the FITC channel (524/40), whereas that from JC-1 aggregates (JC-1_{agg}) and E was collected through the PE channel (585/42). The fluorescence emitted by M540 was detected by the ECD channel (610/20), and that from LD by the APC channel (660/20). The fluorescence emitted by PI was collected through the PC5.5 channel (690/50). A minimum of 5,000 spermatozoa were analyzed per sample.

Sperm viability (SYBR-14/PI)

Sperm viability was evaluated by assessing the integrity of the plasma membrane, following the protocol of Garner & Johnson⁴⁹. For this purpose, the LIVE/DEAD viability kit (Molecular Probes; Eugene, OR, US) was used. Samples were stained with SYBR-14 (31.5 nmol/L) and PI (7.6 $\mu\text{mol/L}$) and incubated at 38 °C for 10 min in the dark. While SYBR-14 is a counterstain, binding to the nuclei of viable and non-viable sperm, PI can only penetrate sperm with damaged plasma membrane⁴⁹. The percentage of SYBR-14-positive and PI-negative (SYBR-14⁺/PI⁻) sperm, which corresponded to viable sperm, was recalculated after subtracting the percentage of debris particles (SYBR-14⁻/PI⁻).

Lipid membrane stability (M540/Yo-Pro-1)

Lipid membrane stability was determined following the protocol of Rathi et al.⁵⁰, with minor modifications. Briefly, samples were stained with M540 (2.5 $\mu\text{mol/L}$) and Yo-Pro-1 (25 nmol/L) at 38 °C in the dark for 10 min. M540 can intercalate into the membrane and emit red fluorescence in conditions of elevated membrane lipid disorder⁵¹. Data were corrected by subtracting the percentage of debris particles (SYBR-14⁻/PI⁻) from the double-negative quadrant (M540⁻/Yo-Pro-1⁻); the percentages of the four sperm subpopulations were then

recalculated. The percentage of viable sperm with low membrane lipid disorder (M540⁻/Yo-Pro-1⁻), known as lipid membrane stability, was the main parameter.

Acrosome integrity (PNA-FITC/PI)

To determine the integrity of the acrosomal membrane, a co-staining with PNA-FITC and PI was performed as described by Nagy et al.⁵². Samples were stained with PNA-FITC (1.17 μmol/L) and PI (5.6 μmol/L) and subsequently incubated at 38 °C in the dark for 10 min. PNA is a lectin that specifically binds the β-galactose residues of the inner acrosomal membrane, which are exposed after the acrosome reaction or when the membrane is not intact; this lectin thus allows for the evaluation of acrosomal integrity⁵³. Data were corrected by subtracting the percentage of debris particles (SYBR-14⁻/PI⁻) from the double-negative quadrant (PNA-FITC⁻/PI⁻); the percentages of the four sperm subpopulations were then recalculated. The percentage of viable sperm with an intact acrosome membrane (PNA-FITC⁻/PI⁻) was used to assess the acrosome integrity.

Intracellular superoxide levels

Intracellular superoxide levels were assessed by following the protocol of Guthrie & Welch⁵⁴. Briefly, sperm were stained with HE (5 μmol/L) and Yo-Pro-1 (31.25 nmol/L) at 38 °C in the dark for 20 min. HE is oxidized into E⁺ by superoxide ions, emitting red fluorescence. Data were corrected by subtracting the percentage of debris particles (SYBR-14⁻/PI⁻) from the double-negative quadrant (E⁺/Yo-Pro-1⁻); the percentages of the four sperm subpopulations were then recalculated. The fluorescence intensity of E⁺ in viable sperm (Yo-Pro-1⁻) was used to evaluate the intracellular superoxide levels. Results are expressed as the ratio between the fluorescence intensity of E⁺ normalized by its respective control.

Intracellular total ROS levels (H₂DCFDA/PI)

Sperm were stained with H₂DCFDA and PI, following the protocol of Guthrie & Welch⁵⁴. Briefly, sperm were incubated with H₂DCFDA (100 μmol/L) at 38 °C in the dark for 20 min. Subsequently, samples were incubated with PI (12 μmol/L) for 5 min under the same conditions. In the presence of ROS within the cells, H₂DCFDA is oxidized to DCF⁺, which emits red fluorescence. Data were corrected by subtracting the percentage of debris particles (SYBR-14⁻/PI⁻) from the double-negative quadrant (DCF⁺/PI⁻); the percentages of the four sperm subpopulations were then recalculated. The DCF⁺ intensity in viable sperm was used to assess total ROS levels. Results are expressed as the ratio between the fluorescence intensity of DCF⁺ normalized by its respective control.

Intracellular Ca²⁺ levels (Fluo4-AM/PI)

Intracellular levels of Ca²⁺ were assessed as described by Harrison et al.⁵⁵, with minor modifications. Samples were co-stained with Fluo4-AM (1.17 μmol/L) and PI (5.6 μmol/L) at 38 °C in the dark for 10 min. Data were corrected by subtracting the percentage of debris particles (SYBR-14⁻/PI⁻) from the double-negative quadrant (Fluo4⁺/PI⁻); the percentages of the four sperm subpopulations were subsequently recalculated. The intensity of Fluo4 fluorescence in viable sperm was used to evaluate the intracellular Ca²⁺ levels, and was expressed as a ratio relative to the corresponding control for each sample.

Mitochondrial membrane potential (JC-1/LIVE/DEAD™ Fixable Far Red)

The evaluation of the mitochondrial membrane potential (MMP) was performed following the protocol described by Llavanera et al.⁵⁶, with minor modifications. Briefly, sperm were stained with JC-1 (750 nmol/L) and LD (1:8,000; v: v) before incubation at 38 °C in the dark for 30 min. At high MMP, JC-1 forms aggregates that emit orange fluorescence (JC-1_{agg}), whereas at low MMP, JC-1 remains in its monomeric form, emitting green fluorescence (JC-1_{mon}). The ratio between JC-1_{agg} and JC-1_{mon} in viable sperm (LD⁻) was calculated and used for assessing the MMP.

Immunoblotting

Sperm were centrifuged at 4,000×g for 5 min, resuspended in PBS, and again centrifuged at the same conditions. The resulting pellets were stored at -80 °C until further use. Upon thawing, sperm were resuspended in 500 μL of lysis buffer (RIPA buffer; Sigma) and then incubated for 45 min, with vortexing every 5 min to facilitate the lysis of cells. Samples were subsequently centrifuged at 14,000×g and 4 °C for 20 min, and the total protein content was quantified using a commercial kit (BioRad; Richmond, CA, USA). Fifteen μL of protein extracts were resuspended in 4× Laemmli Redcutor Buffer (v: v) supplemented with β-mercaptoethanol (10%, v: v), and samples were heated at 95 °C for 5 min. Afterward, samples were loaded in 8–16% Mini-PROTEAN TGX Stain-Free Gels (BioRad), and electrophoresis was conducted at 150 V for 60 min. The Stain-Free method was used to quantify the total protein content in the gel through a G: BOX Chemi XL system (Syngene, Frederick, MD, US). Next, proteins from the gel were transferred onto a PVDF low fluorescence membrane by a Trans-Blot Turbo system (BioRad). Following this, membranes were incubated with blocking buffer (5% BSA in TBS) in agitation for 1 h. Next, membranes were incubated with a primary rabbit anti-SERCA2 antibody (ref. ab3625; Abcam; 1:10,000, v: v) at 4 °C in agitation overnight. Thereafter, membranes were washed thrice in 1× TBS-Tween 20, and incubated with a secondary goat anti-rabbit antibody (ref. P0448; Dako; 1:10,000; v: v) in agitation for 1 h. Finally, membranes were washed five times in 1× TBS-Tween 20 and bands were visualized using a chemiluminescent substrate in a G: BOX Chemi XL system (Syngene).

To confirm the specificity of the primary antibody, a competition assay using a recombinant SERCA2 protein (ref. H00000488-P01; Novus Biologicals; 1:1, v: v, regarding the primary antibody) was run. Besides, a negative control by incubating an additional membrane solely with the secondary antibody was included as a second specificity test for the primary antibody.

Immunofluorescence

The localization of SERCA2 in pig sperm was determined by immunofluorescence. For this purpose, samples were diluted to a concentration of 5×10^6 sperm per mL in PBS, and centrifuged at $600 \times g$ for 5 min and resuspended in PBS twice. Subsequently, sperm were fixed with 4% paraformaldehyde in PBS (ThermoFisher, Kandel, Germany) for 20 min, centrifuged at $600 \times g$ for 5 min and resuspended in PBS. For each sample, a 30 μ L drop was smeared on a separate slide. Sperm were permeabilized in PBS containing 1% Triton X-100 at room temperature for 30 min, and then blocked with 0.02 M glycine in PBS at room temperature for 20 min. Next, samples were washed once with PBS for 5 min, and then incubated with the primary rabbit anti-SERCA2 antibody (ref. ab3625; Abcam; 1:200; v: v) diluted in PBS containing 0.1% BSA, at room temperature overnight. Slides were washed with PBS for 5 min and incubated with a secondary donkey anti-rabbit Alexa Fluor 488 (A21206; ThermoFisher; 1:200; v: v), diluted in PBS containing 0.1% BSA at room temperature for 45 min. Finally, slides were washed five times with PBS and prepared with a mounting medium containing DAPI (Dako, Santa Clara, CA, USA). Samples were observed under a confocal laser-scanning microscope (CLSM, Nikon A1R; Nikon Corp., Tokyo, Japan) with preset acquisition settings, and the images captured were analyzed with the Fiji ImageJ software⁵⁷.

To confirm the primary antibody's specificity, a competition assay was performed using a recombinant SERCA2 protein (ref. H00000488-P01; Novus Biologicals; 2 times in excess with respect to the primary antibody). Additionally, a negative control lacking the primary antibody and incubated solely with the secondary antibody was included. Brightness and contrast were uniformly adjusted across all captured images.

Statistical analyses

Statistical analyses were conducted with SPSS Ver. 27.0 (IBM Corp., Armonk, NY, USA), and results were plotted using GraphPad Prism v.8 (GraphPad software, La Jolla, CA, USA). Data normality and homoscedasticity were tested through the Shapiro-Wilk and Levene tests, respectively. The effects of inhibiting SERCA with Thg on the resilience of sperm to liquid preservation at 17 °C were determined through a linear mixed model. The intra-subjects factor was the time of storage (0, 4, and 10 days), and the inter-subjects factor was the Thg concentration (0, 5, 25, and 50 μ M). Next, pairwise comparisons were established with the post-hoc Bonferroni test. The level of significance was set at $P \leq 0.05$. Data are represented as the mean \pm the standard error of the mean (SEM).

Treatment	Day								
	0		4			10			
	CTRL	CTRL	5 μ M	25 μ M	50 μ M	CTRL	5 μ M	25 μ M	50 μ M
VCL (μ m/s)	84.84 \pm 17.69	70.75 \pm 22.63	86.66 \pm 18.70	81.68 \pm 17.03	74.33 \pm 14.78	46.78 \pm 25.03	50.69 \pm 15.84	45.14 \pm 16.03	46.97 \pm 11.61
VSL (μ m/s)	50.65 \pm 8.91	38.54 \pm 11.27	43.64 \pm 6.30	40.40 \pm 5.99	36.06 \pm 5.84	20.07 \pm 15.79	21.12 \pm 12.57	20.39 \pm 12.28	21.42 \pm 7.91
VAP (μ m/s)	64.71 \pm 11.12	51.94 \pm 17.33	61.81 \pm 10.53	56.54 \pm 7.67	48.94 \pm 7.27	26.74 \pm 15.05	28.89 \pm 12.22	28.33 \pm 14.86	27.88 \pm 7.82
LIN (%)	61.05 \pm 11.07	55.50 \pm 12.11	51.78 \pm 9.43	50.73 \pm 8.98	49.42 \pm 8.56	40.04 \pm 11.05	38.58 \pm 13.51	42.30 \pm 11.59	44.73 \pm 7.77
STR (%)	78.52 \pm 7.29	75.22 \pm 8.56	71.13 \pm 6.59	71.64 \pm 6.67	73.63 \pm 4.99	69.48 \pm 15.00	68.16 \pm 15.32	69.98 \pm 9.63	75.40 \pm 9.68
WOB (%)	77.20 \pm 8.08	73.21 \pm 9.52	72.39 \pm 8.53	70.46 \pm 8.38	66.82 \pm 8.22	56.96 \pm 5.18	55.30 \pm 8.17	59.83 \pm 11.12	59.15 \pm 4.66
ALH (μ m)	2.63 \pm 0.70	2.49 \pm 0.66	2.84 \pm 0.76	2.87 \pm 0.69	2.79 \pm 0.53	2.43 \pm 0.80	2.49 \pm 0.49	2.30 \pm 0.58	2.72 \pm 0.24
BCF (Hz)	8.48 \pm 0.64	8.11 \pm 1.79	8.87 \pm 1.37	8.50 \pm 0.82	7.67 \pm 2.20	4.23 \pm 1.81	4.85 \pm 2.38	4.30 \pm 2.65	4.77 \pm 2.22

Table 1. Effects of inhibiting SERCA with Thg (5, 25, and 50 μ M) on the kinetic parameters of pig sperm stored at 17 °C for 10 days. Data are shown as mean \pm SEM ($n = 7$). Abbreviations: CTRL = control; VCL = curvilinear velocity; VSL = straight-line velocity; VAP = average-path velocity; LIN = linearity; STR = straightness; WOB = wobble; ALH = amplitude of lateral head displacement; BCF = beat-cross frequency.

Data availability

The datasets generated during and/or analyzed during the current study are available from the corresponding author on reasonable request.

Received: 15 November 2024; Accepted: 23 January 2025

Published online: 04 February 2025

References

- Waberski, D., Riesenbeck, A., Schulze, M., Weitze, K. F. & Johnson, L. Application of preserved boar semen for artificial insemination: Past, present and future challenges. *Theriogenology* **137**, 2–7. <https://doi.org/10.1016/j.theriogenology.2019.05.030> (2019).
- Yeste, M. Sperm cryopreservation update: Cryodamage, markers, and factors affecting the sperm freezability in pigs. *Theriogenology* **85**, 47–64. <https://doi.org/10.1016/j.theriogenology.2015.09.047> (2016).
- Yáñez-Ortiz, I., Catalán, J., Rodríguez-Gil, J. E., Miró, J. & Yeste, M. Advances in sperm cryopreservation in farm animals: Cattle, horse, pig and sheep. *Anim. Reprod. Sci.* **246**, 106904. <https://doi.org/10.1016/j.anireprosci.2021.106904> (2022).
- Pursel, V. G., Johnson, L. A. & Schulman, L. L. Effect of dilution, seminal plasma and incubation period on cold shock susceptibility of Boar Spermatozoa. *J. Anim. Sci.* **37**, 528–531. <https://doi.org/10.2527/jas1973.372528x> (1973).

5. Yeste, M. State-of-the-art of boar sperm preservation in liquid and frozen state. *Anim. Reprod.* **14**, 69–81. <https://doi.org/10.21451/1984-3143-AR895> (2017).
6. Alasmari, W. et al. Ca²⁺ signals generated by CatSper and Ca²⁺ stores regulate different behaviors in human Sperm*. *J. Biol. Chem.* **288**, 6248–6258. <https://doi.org/10.1074/jbc.M112.439356> (2013).
7. Brukman, N. G. et al. Tyrosine phosphorylation signaling regulates ca²⁺ entry by affecting intracellular pH during human sperm capacitation. *J. Cell. Physiol.* **234**, 5276–5288. <https://doi.org/10.1002/jcp.27337> (2019).
8. Mata-Martínez, E. et al. Role of calcium oscillations in sperm physiology. *Biosystems* **209**, 104524. <https://doi.org/10.1016/j.biosystems.2021.104524> (2021).
9. Sushadi, P. S. et al. Arresting calcium-regulated sperm metabolic dynamics enables prolonged fertility in poultry liquid semen storage. *Sci. Rep.* **13**, 21775. <https://doi.org/10.1038/s41598-023-48550-2> (2023).
10. Ren, D. et al. A sperm ion channel required for sperm motility and male fertility. *Nature* **413**, 603–609. <https://doi.org/10.1038/35098027> (2001).
11. Sakata, Y. et al. Ca_v2.3 (α_{1E}) ca²⁺ channel participates in the control of sperm function. *FEBS Lett.* **516**, 229–233. [https://doi.org/10.1016/S0014-5793\(02\)02529-2](https://doi.org/10.1016/S0014-5793(02)02529-2) (2002).
12. Dragileva, E., Rubinstein, S. & Breitbart, H. Intracellular Ca²⁺-Mg²⁺-ATPase regulates calcium influx and Acrosomal Exocytosis in Bull and Ram Spermatozoa. *Biol. Reprod.* **61**, 1226–1234. <https://doi.org/10.1095/biolreprod61.5.1226> (1999).
13. Ho, H.-C., Granish, K. A. & Suarez, S. S. Hyperactivated motility of bull sperm is triggered at the Axoneme by Ca²⁺ and not cAMP. *Dev. Biol.* **250**, 208–217. <https://doi.org/10.1006/dbio.2002.0797> (2002).
14. Luconi, M., Krausz, C., Forti, G. & Baldi, E. Extracellular calcium negatively modulates tyrosine phosphorylation and tyrosine kinase activity during Capacitation of Human Spermatozoa. *Biol. Reprod.* **55**, 207–216. <https://doi.org/10.1095/biolreprod55.1.207> (1996).
15. Shabtay, O. & Breitbart, H. CaMKII prevents spontaneous acrosomal exocytosis in sperm through induction of actin polymerization. *Dev. Biol.* **415**, 64–74. <https://doi.org/10.1016/j.ydbio.2016.05.008> (2016).
16. Hachem, A. et al. PLC ζ is the physiological trigger of the Ca²⁺ oscillations that induce embryogenesis in mammals but conception can occur in its absence. *Development* **144**, 2914–2924. <https://doi.org/10.1242/dev.150227> (2017).
17. Saunders, C. M. et al. PLC ζ : a sperm-specific trigger of Ca²⁺ oscillations in eggs and embryo development. *Development* **129**, 3533–3544. <https://doi.org/10.1242/dev.129.15.3533> (2002).
18. Garriga, F., Martínez-Hernández, J., Gerrer-Velasco, N., Rodríguez-Gil, J. E. & Yeste, M. Voltage-dependent anion channels are involved in the maintenance of pig sperm quality during liquid preservation. *Theriogenology* **224**, 26–33. <https://doi.org/10.1016/j.theriogenology.2024.05.003> (2024).
19. Pavaneli, A. P. P. et al. The presence of seminal plasma during liquid storage of pig spermatozoa at 17°C modulates their ability to elicit in vitro capacitation and trigger acrosomal exocytosis. *Int. J. Mol. Sci.* **21**, 4520. <https://doi.org/10.3390/ijms21124520> (2020).
20. Pinart, E., Yeste, M., Puigmulé, M., Barrera, X. & Bonet, S. Acrosin activity is a suitable indicator of boar semen preservation at 17°C when increasing environmental temperature and radiation. *Theriogenology* **80**, 234–247. <https://doi.org/10.1016/j.theriogenology.2013.04.001> (2013).
21. Periasamy, M. & Kalyanasundaram, A. SERCA pump isoforms: Their role in calcium transport and disease. *Muscle Nerve.* **35**, 430–442. <https://doi.org/10.1002/mus.20745> (2007).
22. Lawson, C., Dorval, V., Goupil, S. & Leclerc, P. Identification and localisation of SERCA 2 isoforms in mammalian sperm. *MHR: Basic. Sci. Reproductive Med.* **13**, 307–316. <https://doi.org/10.1093/molehr/gam012> (2007).
23. Lytton, J., Westlin, M. & Hanley, M. R. Thapsigargin inhibits the sarcoplasmic or endoplasmic reticulum Ca-ATPase family of calcium pumps. *J. Biol. Chem.* **266**, 17067–17071. [https://doi.org/10.1016/S0021-9258\(19\)47340-7](https://doi.org/10.1016/S0021-9258(19)47340-7) (1991).
24. Sehgal, P. et al. Inhibition of the sarco/endoplasmic reticulum (ER) Ca²⁺-ATPase by thapsigargin analogs induces cell death via ER Ca²⁺ depletion and the unfolded protein response. *J. Biol. Chem.* **292**, 19656–19673. <https://doi.org/10.1074/jbc.M117.796920> (2017).
25. Meizel, S. & Turner, K. O. Initiation of the human sperm acrosome reaction by thapsigargin. *J. Exp. Zool.* **267**, 350–355. <https://doi.org/10.1002/jez.1402670312> (1993).
26. Rossato, M., Di Virgilio, F., Rizzuto, R., Galeazzi, C. & Foresta, C. Intracellular calcium store depletion and acrosome reaction in human spermatozoa: role of calcium and plasma membrane potential. *Mol. Hum. Reprod.* **7**, 119–128. <https://doi.org/10.1093/molehr/7.2.119> (2001).
27. Williams, K. M. & Ford, W. C. L. Effects of Ca-ATPase inhibitors on the intracellular calcium activity and motility of human spermatozoa. *Int. J. Androl.* **26**, 366–375. <https://doi.org/10.1111/j.1365-2605.2003.00438.x> (2003).
28. Kim, J.-C. et al. Effects of Cryopreservation on Ca²⁺ signals Induced by membrane depolarization, Caffeine, Thapsigargin and Progesterone in Boar Spermatozoa. *Mol. Cells.* **26**, 558–565. [https://doi.org/10.1016/S1016-8478\(23\)14037-4](https://doi.org/10.1016/S1016-8478(23)14037-4) (2008).
29. Harayama, H., Okada, K. & Miyake, M. Involvement of cytoplasmic free calcium in boar sperm: Head-to-head agglutination induced by a cell-permeable cyclic adenosine monophosphate analog. *J. Androl.* **24**, 91–99 (2003).
30. Lytton, J. & MacLennan, D. H. Molecular cloning of cDNAs from human kidney coding for two alternatively spliced products of the cardiac Ca²⁺-ATPase gene. *J. Biol. Chem.* **263**, 15024–15031 (1988).
31. Jaskulska, A., Janecka, A. E. & Gach-Janczak, K. Thapsigargin—from traditional medicine to anticancer drug. *Int. J. Mol. Sci.* **22**, 4. <https://doi.org/10.3390/ijms22010004> (2020).
32. Bejarano, I. et al. Caspase 3 activation in human spermatozoa in response to hydrogen peroxide and progesterone. *Fertil. Steril.* **90**, 1340–1347. <https://doi.org/10.1016/j.fertnstert.2007.08.069> (2008).
33. Engel, K. M., Springsguth, C. H. & Grunewald, S. What happens to the unsuccessful spermatozoa? *Andrology* **6**, 335–344. <https://doi.org/10.1111/andr.12467> (2018).
34. Keshtgar, S. & Ghani, E. Impact of calcium and reactive oxygen species on human sperm function: role of <sc>NOX5. *Andrologia* **54**. <https://doi.org/10.1111/and.14470> (2022).
35. Llanos, M. N. Thapsigargin stimulates acrosomal exocytosis in hamster spermatozoa. *Mol. Reprod. Dev.* **51**, 84–91. [https://doi.org/10.1002/\(SICI\)1098-2795\(199809\)51:1<84::AID-MRD10>3.0.CO;2-U](https://doi.org/10.1002/(SICI)1098-2795(199809)51:1<84::AID-MRD10>3.0.CO;2-U) (1998).
36. Costello, S. et al. Ca²⁺-stores in sperm: Their identities and functions. *Reproduction* **138**, 425–437. <https://doi.org/10.1530/REP-09-0134> (2009).
37. Herrick, S. B. et al. The acrosomal vesicle of mouse sperm is a calcium store. *J. Cell. Physiol.* **202**, 663–671. <https://doi.org/10.1002/jcp.20172> (2005).
38. O'Toole, C. M. B., Arnoult, C., Darszon, A., Steinhardt, R. A. & Florman, H. M. Ca²⁺ entry through Store-operated channels in mouse sperm is initiated by Egg ZP3 and drives the Acrosome reaction. *Mol. Biol. Cell.* **11**, 1571–1584. <https://doi.org/10.1091/mcb.11.5.1571> (2000).
39. Bernecic, N. C., Gadella, B. M., Leahy, T. & de Graaf, S. P. Novel methods to detect capacitation-related changes in spermatozoa. *Theriogenology* **137**, 56–66. <https://doi.org/10.1016/j.theriogenology.2019.05.038> (2019).
40. Harayama, H. Flagellar hyperactivation of bull and boar spermatozoa. *Reprod. Med. Biol.* **17**, 442–448. <https://doi.org/10.1002/rmb2.12227> (2018).
41. Prakriya, M. & Lewis, R. S. Store-operated calcium channels. *Physiol. Rev.* **95**, 1383–1436. <https://doi.org/10.1152/physrev.00020.2014> (2015).
42. Strange, K., Yan, X., Lorin-Nebel, C. & Xing, J. Physiological roles of STIM1 and Orai1 homologs and CRAC channels in the genetic model organism *Caenorhabditis elegans*. *Cell. Calcium.* **42**, 193–203. <https://doi.org/10.1016/j.ceca.2007.02.007> (2007).

43. Wang, Y. et al. ORAI AND TRPC channels in the control of calcium entry signals in smooth muscle. *Clin. Exp. Pharmacol. Physiol.* **35**, 1127–1133. <https://doi.org/10.1111/j.1440-1681.2008.05018.x> (2008).
44. Davis, F. M. et al. Male infertility in mice lacking the store-operated Ca²⁺ channel Orai1. *Cell. Calcium*. **59**, 189–197. <https://doi.org/10.1016/j.ceca.2016.02.007> (2016).
45. Rossi, A., Pizzo, P. & Filadi, R. Calcium, mitochondria and cell metabolism: A functional triangle in bioenergetics. *Biochimica et Biophysica Acta (BBA). Mol. Cell. Res.* **1866**, 1068–1078. <https://doi.org/10.1016/j.bbamcr.2018.10.016> (2019).
46. Sabeti, P., Pourmasumi, S., Rahiminia, T., Akyash, F. & Talebi, A. R. Etiologies of sperm oxidative stress. *Int. J. Reprod. Biomed.* **14**, 231–240. <https://doi.org/10.29252/ijrm.14.4.231> (2016).
47. Mateo-Otero, Y., Llavanera, M., Torres-Garrido, M. & Yeste, M. Embryo development is impaired by sperm mitochondrial-derived ROS. *Biol. Res.* **57**, 5. <https://doi.org/10.1186/s40659-024-00483-4> (2024).
48. Li, X. et al. Calcium regulates motility and protein phosphorylation by changing cAMP and ATP concentrations in boar sperm in vitro. *Anim. Reprod. Sci.* **172**, 39–51. <https://doi.org/10.1016/j.anireprosci.2016.07.001> (2016).
49. Garner, D. L. & Johnson, L. A. Viability Assessment of mammalian sperm using SYBR-14 and Propidium Iodide1. *Biol. Reprod.* **53**, 276–284. <https://doi.org/10.1095/biolreprod53.2.276> (1995).
50. Rathi, R., Colenbrander, B., Bevers, M. M. & Gadella, B. M. Evaluation of in vitro capacitation of stallion spermatozoa1. *Biol. Reprod.* **65**, 462–470. <https://doi.org/10.1095/biolreprod65.2.462> (2001).
51. Williamson, P., Mattocks, K. & Schlegel, R. A. Merocyanine 540, a fluorescent probe sensitive to lipid packing. *Biochimica et Biophysica Acta (BBA). Biomembr.* **732**, 387–393. [https://doi.org/10.1016/0005-2736\(83\)90055-X](https://doi.org/10.1016/0005-2736(83)90055-X) (1983).
52. Nagy, S., Jansen, J., Topper, E. K. & Gadella, B. M. A triple-stain Flow Cytometric Method to assess plasma- and acrosome-membrane Integrity of Cryopreserved bovine sperm immediately after thawing in Presence of Egg-Yolk Particles1. *Biol. Reprod.* **68**, 1828–1835. <https://doi.org/10.1095/biolreprod.102.011445> (2003).
53. Mortimer, D., Curtis, E. F. & Miller, R. G. Specific labelling by peanut agglutinin of the outer acrosomal membrane of the human spermatozoon. *Reproduction* **81**, 127–135. <https://doi.org/10.1530/jrf.0.0810127> (1987).
54. Guthrie, H. D. & Welch, G. R. Determination of intracellular reactive oxygen species and high mitochondrial membrane potential in Percoll-treated viable boar sperm using fluorescence-activated flow cytometry1. *J. Anim. Sci.* **84**, 2089–2100. <https://doi.org/10.2527/jas.2005-766> (2006).
55. Harrison, R. A. P., Mairet, B. & Miller, N. G. A. Flow cytometric studies of bicarbonate-mediated Ca²⁺ influx in boar sperm populations. *Mol. Reprod. Dev.* **35**, 197–208. <https://doi.org/10.1002/mrd.1080350214> (1993).
56. Llavanera, M. et al. Deactivation of the JNK pathway by GSTP1 is essential to maintain sperm functionality. *Front. Cell. Dev. Biol.* **9**. <https://doi.org/10.3389/fcell.2021.627140> (2021).
57. Schindelin, J. et al. Fiji: An open-source platform for biological-image analysis. *Nat. Methods.* **9**, 676–682 (2012).

Acknowledgements

Not applicable.

Author contributions

FG, ML and MY conceived the research and designed the experiments. FG, JM-H and AP-B conducted laboratory analysis. FG, ML and MY participated in the discussion of data. FG wrote the Manuscript. ML and MY revised and edited the Manuscript. All authors contributed to the finalized Manuscript, read and approved the final version.

Funding

This study was supported by the Ministry of Science, Innovation and Universities, Spain (grants: PID2020-113320RB-I00 and PRE2021-098896), the European Union-Next Generation EU Funds (University of Murcia, Margarita Salas Scheme 181/MSJD/22), the Regional Government of Catalonia (2021-SGR-0900), and the Catalan Institution for Research and Advanced Studies (ICREA).

Declarations

Ethics approval and consent to participate

Not applicable.

Consent for publication

Not applicable.

Competing interests

The authors declare no competing interests.

Additional information

Supplementary Information The online version contains supplementary material available at <https://doi.org/10.1038/s41598-025-88012-5>.

Correspondence and requests for materials should be addressed to M.L. or M.Y.

Reprints and permissions information is available at www.nature.com/reprints.

Publisher's note Springer Nature remains neutral with regard to jurisdictional claims in published maps and institutional affiliations.

Open Access This article is licensed under a Creative Commons Attribution-NonCommercial-NoDerivatives 4.0 International License, which permits any non-commercial use, sharing, distribution and reproduction in any medium or format, as long as you give appropriate credit to the original author(s) and the source, provide a link to the Creative Commons licence, and indicate if you modified the licensed material. You do not have permission under this licence to share adapted material derived from this article or parts of it. The images or other third party material in this article are included in the article's Creative Commons licence, unless indicated otherwise in a credit line to the material. If material is not included in the article's Creative Commons licence and your intended use is not permitted by statutory regulation or exceeds the permitted use, you will need to obtain permission directly from the copyright holder. To view a copy of this licence, visit <http://creativecommons.org/licenses/by-nc-nd/4.0/>.

© The Author(s) 2025